High-reflectivity high-contrast grating focusing reflector on silicon-on-insulator wafer*

Wenjing Fang(房文敬)[1,2], Yongqing Huang(黄永清)[1,2,†], Xiaofeng Duan(段晓峰)[1,2], Kai Liu(刘凯)[1,2], Jiarui Fei(费嘉瑞)[1,2], and Xiaomin Ren(任晓敏)[1,2]

[1] *Institute of Information Photonics and Optical Communications, Beijing University of Posts and Telecommunications, Beijing* 100876, *China*
[2] *State Key Laboratory of Information Photonics and Optical Communications, Beijing University of Posts and Telecommunications, Beijing* 100876, *China*

(Received 7 April 2016; revised manuscript received 20 July 2016; published online 30 September 2016)

A high-contrast grating (HCG) focusing reflector providing phase front control of reflected light and high reflectivity is proposed and fabricated. Basic design rules to engineer this category of structures are given in detail. A 1550 nm TM polarized incident light of 11.86 mm in focal length and 0.8320 in reflectivity is obtained in experiment. The wavelength dependence of the fabricated HCGs from 1530 nm to 1580 nm is also tested. The test results show that the focal length is in the range of 11.81–12 mm, which is close to the designed focal length of 15 mm. The reflectivity is almost above 0.56 within a bandwidth of 50 nm. At a distance of 11.86 mm, the light is focused to a round spot with the highest concentration, which is much smaller than the size of the incident beam. The FWHM of the reflected light beam decreases to 120 nm, and the intensity increases to 1.18.

Keywords: gratings, reflectors, polarization

PACS: 42.79.Dj, 42.79.Fm, 42.68.Mj **DOI:** 10.1088/1674-1056/25/11/114213

1. Introduction

High-contrast grating (HCG) used as a reflector or a lens in vertical surface emitting lasers (VCESELs) and reflection enhanced photodetectors has recently great attention as an alternative to distributed Bragg reflectors (DBRs).[1–5] A HCG is a subwavelength structure with a high contrast of refractive indexes that can provide a high reflectivity or a high transmittance over a broad bandwidth.[6,7] This is an excellent optical property for periodic HCGs, which can be used to design for broadband reflectors,[8,9] high-Q resonators,[10] filters,[11,12] polarizing beam splitter,[13] etc., because the elimination of nonzero diffraction orders increases coupling efficiency. Another important property of non-periodic HCG is that it can be designed to realize focusing ability and steering ability with high reflectivity or high transmissivity by phase front manipulation has been proposed, which is a significant development in the application of HCG.[14–18] So far, several types of focusing reflectors based on non-periodic HCGs aiming at focusing reflectors with high reflectivity have been studied, which includes stripe type, ring type and 2D blocky type.[19] However, most of these reflectors have only been numerically studied and have rarely been experimentally studied. Furthermore, there has been no detailed experimental demonstration for high reflectance and focusing ability. A planar focusing reflector composed of non-periodic HCGs on silicon-on-insulator (SOI) wafer is presented in this paper. We have motivated the experimental investigation of the focusing ability properties of non-periodic stripe HCGs. This reflector not only has good beam focusing ability but also maintains a high reflectivity. In addition, SOI wafer is more suitable for fabrication of HCGs and fabrication process is completely compatible with standard complementary metal oxide semiconductor (CMOS) technology. Similarly, HCGs are more compact and inexpensive than dielectric stacks in terms of fabrication and show good performance and long-term reliability.

In this paper, the beam focusing ability of non-periodic HCGs to control the phase front of reflected light is investigated and the design rules to realization of practical structure are formulated. A non-periodic HCG reflector with a focal length of 15 mm is fabricated and experimentally tested. Experimental results show that the focal length of mirror is 11.86 mm and the reflectivity is up to 0.8320 for TM polarization at wavelength of 1550 nm. The focal length and reflectivity at wavelength range of 1530–1580 nm are also measured, their focal lengths are in the range from 11.81 to 12 mm, and the reflectivity is mostly above 0.56 within a bandwidth of 50 nm. Furthermore, intensity distributions at the focal spot and the original Gaussian intensity profile are recorded by CCD camera. The FWHM of the incident beam decreases from 235 μm to 120 μm. The intensity increases by a factor

*Project supported by the National Natural Science Foundation of China (Grant Nos. 61274044, 61574019 and 61020106007), the National Basic Research Program of China (Grant No. 2010CB327600), the Specialized Research Fund for the Doctoral Program of Higher Education of China (Grant No. 20130005130001), the Natural Science Foundation of Beijing, China (Grant No. 4132069), the Key International Science and Technology Cooperation Project of China (Grant No. 2011RR000100), the 111 Project of China (Grant No. B07005), and the Program for Changjiang Scholars and Innovative Research Team in Universities of China (Grant No. IRT0609).

†Corresponding author. E-mail: yqhuang@bupt.edu.cn

© 2016 Chinese Physical Society and IOP Publishing Ltd

of 1.18 compared to the input beam intensity.

2. Methods

2.1. Theoretical background

When a light wave is illuminated on a periodic HCG, a phase variation will be developed along the x axis, which is spatially dependent on the HCG structure parameters at a certain wavelength. The structure parameters that determine the phase shift are grating period (Λ), width of grating bar (s) grating thickness (t_g), low-refractive index material thickness (t_l) and the refractive indexes. Changing the grating thickness to control phase front is not feasible due to the multiple etching step that it requires. Hence, only variations of period and width of grating bar are considered. When the grating period and grating bar width are locally changed, the properties of reflected beam, such as phase and reflectivity, will gradually adapt to these variation. If the phase response profile of the reflected light at the reflected plane is parabolic, then the reflected beam can be focused to a spot as shown in Fig. 1(a). The total phase shift $\Delta\Phi$ is achieved by designing the HCG structure of width d, as shown in Fig. 1(b).[15–19]

$$\Phi(x) = \frac{2\pi}{\lambda}\left(\sqrt{x^2 + f_x^2} - f_x\right) + \Phi_0, \tag{1}$$

where f_x is the focal length, λ is the wavelength, and Φ_0 is the phase shift at $x = 0$. If the phase $\Phi(x)$ is more than 2π, then it can be mapped to an equivalent value between 0 and 2π.

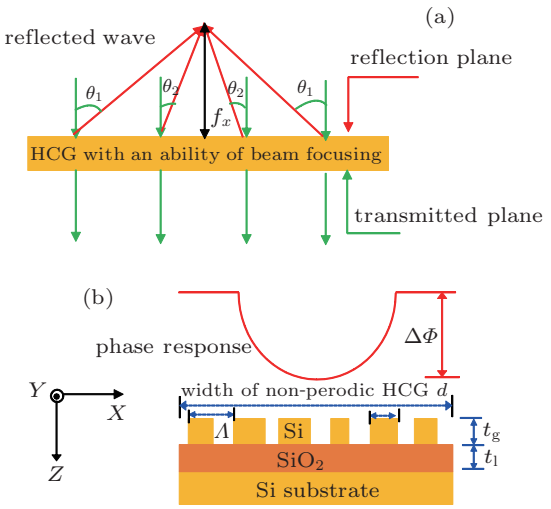


Fig. 1. (color online) Structure layout and parameters. (a) Schematic diagram of the HCG structure proposed under TM polarized illumination. (b) Schematic of the investigated non-periodic HCGs with a parabolic phase response.

2.2. Design

For the design of a focusing non-periodic HCGs, it is important to choose proper grating parameters (period and width of grating bars) that achieve a particular phase profile along the x axis. Firstly, by changing the period and width of grating bars, we obtain reflectivity and phase shift of reflected light as a function of grating period (Λ) and the width of grating bar (s) of periodic HCGs for a certain grating thickness using the rigorous coupled wave analysis (RCWA) simulation method,[20] as shown in Fig. 2. Figure 2(a) shows the reflectivity of the reflected light. Figure 2(b) exhibits that the phase of the reflected light covers a full 2π range of variation within the high reflectivity region. Then, the above simulation results are taken as look-up tables to select a set of (Λ_n, s_n) which can achieve a high reflectivity and a gradually changed phase shift range from 0 radian to 2π radian. These data will be the look-up table that is used to select the grating unit according to the goal phase shift distribution from Eq. (1).

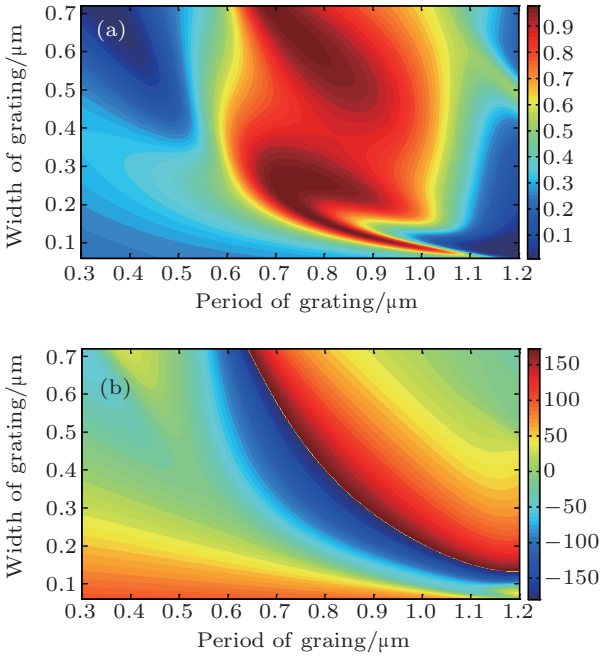


Fig. 2. (color online) (a) Reflectivity and (b) phase shift of reflected light as a function of grating period and the grating bar width of periodic grating at wavelength of 1550 nm.

For example, a non-periodic HCG focusing reflector with a focal length of 300 μm for the TM polarized light at an incident wavelength of 1550 nm is designed. The performance of the focusing element is evaluated by using COMSOL finite-element method (FEM) numerical simulation.[21] The design of the device requires a total phase variation of 9.78π from center to edge, as shown in Fig. 3(a). E-field intensity on the reflected plane is plotted in Fig. 3(b). Most of the reflected wave is focused to a spot of 295 μm, which is in agreement with 300 μm. This small deviation is caused by discrete phase distribution, and the total reflectivity of 0.92 is obtained by calculation. The phase of numerical simulation at the reflection plane are obtained by the modulation of period and width using the reflectance of Fig. 2(a) as shown in Fig. 3(c), which is in agreement with the ideal phase profile shown in Fig. 3(a). With all of these desirable attributes, the designed mirror shows excellent focusing ability.

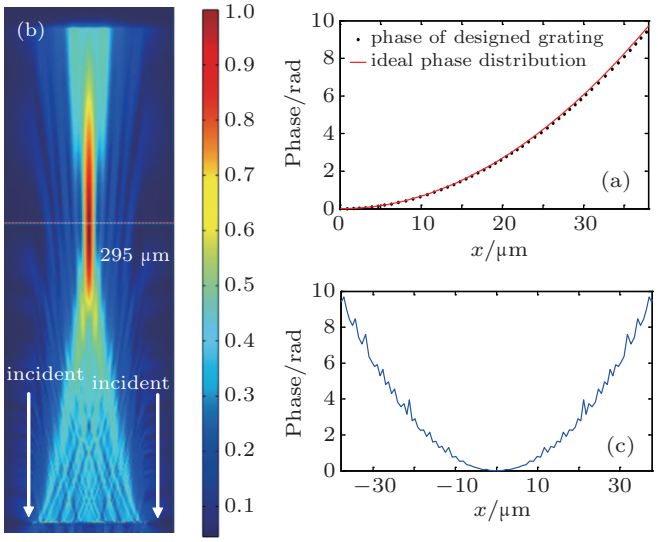


Fig. 3. (color online) (a) Phase distribution of a non-periodic HCGs focusing reflector. (b) E-field intensity distribution for a non-periodic HCGs focusing reflector. (c) Obtained phase at the reflected plane.

3. Fabrication

In order to facilitate the measurement of the reflected light, the non-periodic HCGs structure with a small numerical aperture (NA is 0.0167) and a relatively long focal length of 15 mm was fabricated on a SOI wafer. An EB resist (ZEP520) was spin-coated on a SOI wafer. The grating patterns were defined by electron-beam lithography. Then, using the EB resist as a mask, the silicon grooves were formed by inductively coupled-plasma (ICP) etching using C_4F_8 and SF_6. The etching depth was controlled by the etching time. The etching rate of the silicon was 21 nm/min. Finally, the residual EB resist was removed with a 1:1 solution of H_2SO_4 and H_2O_2. The gratings were etched 500 nm into the top silicon layer and the total structure is a square of 500 μm ×500 μm. The designed reflector requires a total phase variation of 22.8851π from center to edge, which is obtained through the spatial modulation of period and duty cycle, similar to Fig. 3(a). The SEM micrographs of fabricated structures are shown in Fig. 4, together with the scanning electron microscope images of silicon grooves at a location.

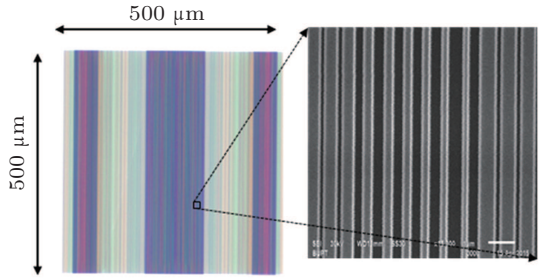


Fig. 4. (color online) Optical microscope picture of a fabricated non-periodic HCGs reflector. The groove width in a location is shown in the SEM image in the inset.

4. Results and discussion

4.1. High reflectivity of focusing reflector

The reflectance of HCG reflector for TM polarization at wavelength of 1550 nm was measured. The measurement setup used to proof HCGs with focusing ability is depicted in Fig. 5. An Anritsu Tunics SCL tunable laser with a single-mode fiber pigtail was used as the light source. The laser beam's polarization state is set to TM using a polarization controller (PC) and it is then coupled to a three port polarization maintaining optical circulator (insertion loss is less than 0.7 dB) with wavelength range from 1530 nm to 1580 nm. The non-periodic HCG was illuminated by an input beam from port 2 through the lensed fiber with normal incidence. The reflectance data was collected using an optical power meter from port 3. To facilitate the statistics and observation, a computer is connected by a GPIB controller to the tunable laser and the optical power meter. A Python script will automatically scan and record the wavelength and reflected power on the computer. Finally, the wavelength and optical power curve were drawn according to the received data.

Experimental results are summarized in Fig. 6. The measured intensity along the z axis at $x = 0$ is shown in Fig. 6(a), and the intensity along the x axis direction at some different z points is displayed in Fig. 6(b). As illustrated in Fig. 6(a), the peak intensity increases with the z direction to reach a maximum at 11.86 mm and it then decreases. The focal length is calculated to be 11.86 mm, close to the design value of 15 mm. The differences between the designed value and measured value may have several reasons. First of all, the error is caused by the discrete phase. Furthermore, some errors are introduced by the measurement setup. The error of the fiber position was ±0.5 μm. The plot in Fig. 6(b) shows that measurement results are fitted to a Gaussian profile. It can be seen that the highest intensity and the narrowest FWHM appear at the focal length. Using these parameters, the total reflectivity of the reflector at the focusing plane is 0.8320 by calculation, which is lower than the designed value of 97%. This may be contributed to by proximity effects in the electron-beam lithography step, as well as the surface roughness of the silicon grooves evidently seen in Fig. 4.[14]

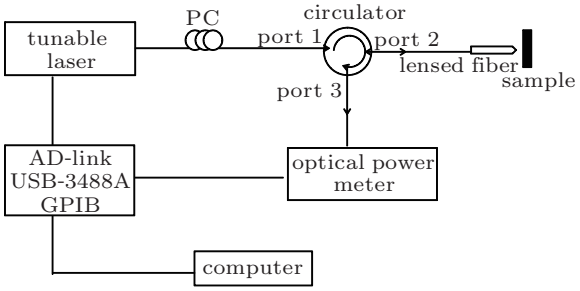


Fig. 5. The setup used to test the HCG structure with focusing ability.

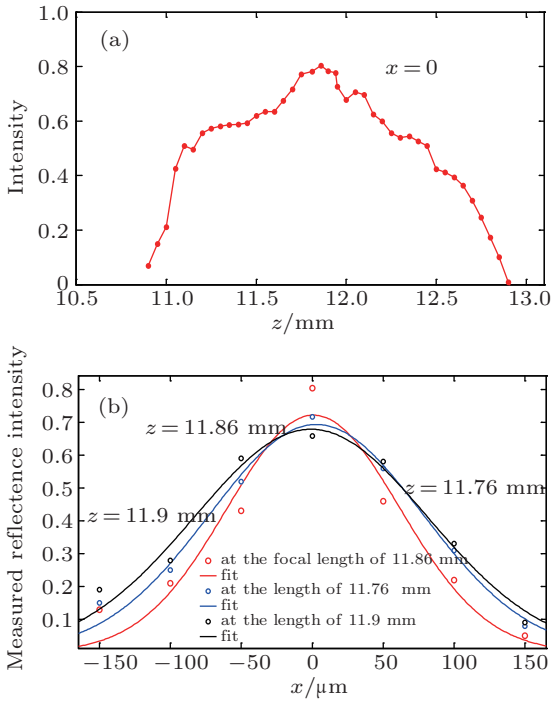


Fig. 6. (color online) (a) Measured intensity at different positions in the z direction. (b) Measurement results (points) and the fitting results (continuous lines) at different positions in the x direction.

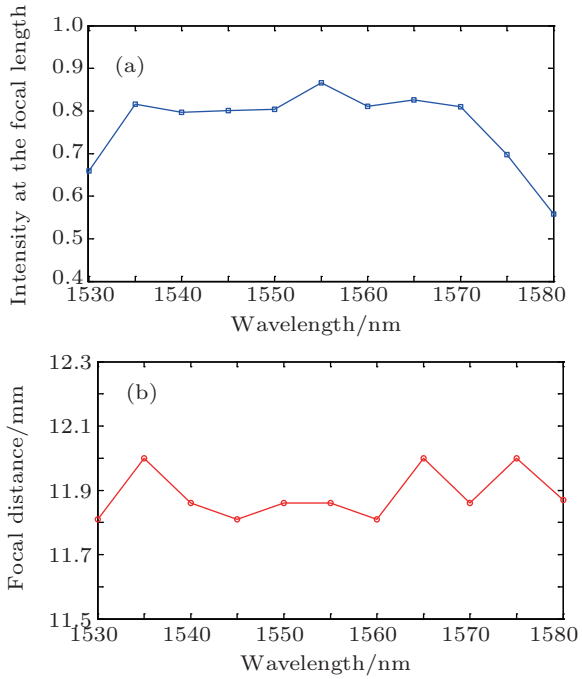


Fig. 7. (color online) Intensity of the focused spot, and the focal distance, for the reflected beam for TM versus wavelength for 1530–1580 nm. (a) Intensity. (b) Focal distance.

The wavelength dependence of the fabricated structure were also tested from 1530 nm to 1580 nm. The intensity of the focused spot and the focal distance for the reflected beams with TM polarization versus wavelength for 1530–1580 nm are plotted in Figs. 7(a)–7(b), respectively. The reflectivity of the focused reflected beam is mostly above 0.56 by calculation, and the focus length is between 11.81 mm and 12 mm within a bandwidth of 50 nm. The test results show that the fabricated grating has a good focusing ability with a high reflectivity at a relatively wide bandwidth. We believe that the focal length and reflectivity will be much closer to the designed value after optimization in the fabrication procedure.

4.2. Focusing effect

Focusing properties of the non-periodic reflector were experimentally studied. The surface of the HCG wafer was illuminated by the 1550 nm input beam, as shown in Fig. 8.

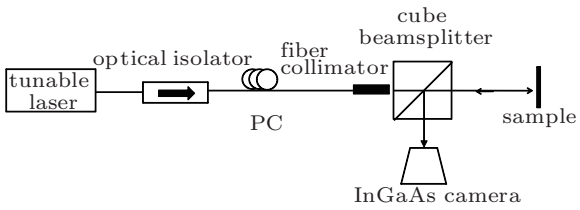


Fig. 8. Schematic of the focusing effect demonstration.

The focal length of 11.86 mm is obtained at wavelength of 1550 nm from the experimental results shown Fig. 5. In order to better illustrate the focusing property, intensity profiles of incident light and focal spot are obtained by an InGaAs CCD camera respectively, as shown in Fig. 8. Here, a polarization controller (PC) was used to switch the polarization of the light injected into the sample between TE and TM polarizations. A fiber collimator (reflectivity: 0.5%) was used to generate a large diameter beam approximately matching the size of the fabricated structure. The grating was illuminated by the transmitted light through a cube beam splitter with 50:50 split ratio. The reflected beam from HCG was again separated from the incoming beam by the cube beam splitter. Then, an InGaAs CCD camera was deployed to record the intensity distribution of the reflected beam.

Figure 9(a) shows the intensity distribution of the incident light in which the waist of incident light is about 300 μm. The plot in Fig. 9(b) shows the intensity profile at the focal spot. It can be seen that the focusing reflector reduces the beam spot size at the focal spot. The FWHM is 120 μm compared to 235 μm of the incident beam. The peak intensity increases by a factor of 1.18 compared to incident beam intensity. The three factors may contribute to the loss. First, a part of loss is attributed to transmission from substrate backside interface. Second, a portion is scattered by the random roughness of the etched silicon posts. Finally, most of loss is attributed to the cube beam-splitter. Based on the principle of a cube beam-splitter, the factor is that the reflectance from the grating again passes through the cube beam-splitter. The intensity of the measured reflectance is 50% smaller than incident light. Since the data in Fig. 9(b) is measured directly from the CCD and

does not change, the peak intensity of reflectance should be twice the original measured data (see Fig. 9(b)).

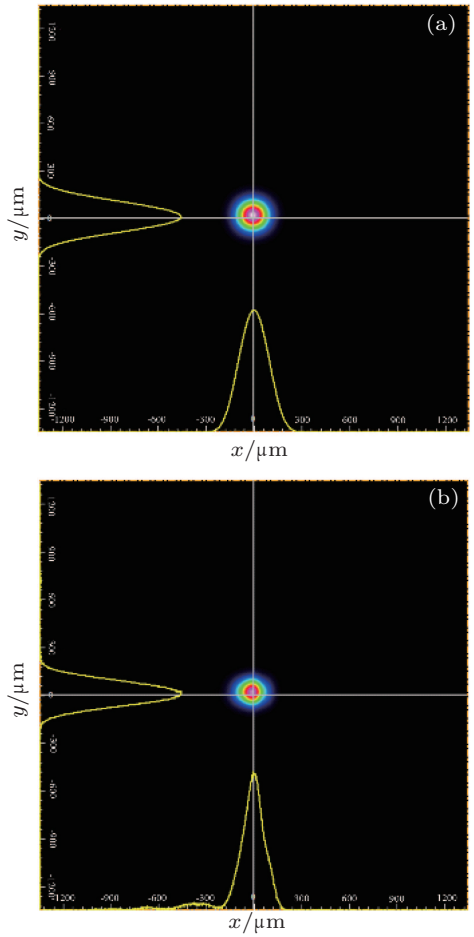


Fig. 9. (color online) Intensity profiles of (a) incident light and (b) focal spot.

5. Conclusions

In conclusion, a high contrast grating (HCG) focusing reflector patterned on a SOI wafer is demonstrated. Basic design rules to obtain focusing performance by phase front control are explained in detail. Experimental results of fabricated non-periodic HCGs show the focal length of 11.86 mm and the reflectance of 0.8320 at 1550 nm wavelength for TM polarization. Reflectivity of the focused spot and the focal distance for the reflected beam were also tested. The intensity of the focused reflected beams is above 0.56 of the incident beam, and the focus length is close to the designed value of 15 mm within a bandwidth of 50 nm. Furthermore, the FWHM of the input beam decreases from 235 nm to 120 nm. The intensity increases to 1.18 compared to input beam intensity. With all of these good properties, such reflectors can be integrated with photodetectors, solar cells, microscopes, telescopes, and VCSELs to radically enhance their performance.

References

[1] Chase C, Rao Y, Hofmann W and Chang-Hasnain C J 2010 *Opt. Express* **18** 15461
[2] Zhou Y, Huang M C Y and Chang-Hasnain C J 2008 *Opt. Express* **16** 14221
[3] Gründl T, Zogal K, Debernardi P, Müller M, Grasse C, Geiger K, Meyer R, Böhm G, Amann M, Küppers F and Meissner P 2013 *IEEE Photon. Technol. Lett.* **25** 841
[4] Duan X F, Huang Y Q, Ren X M, Shang Y F, Fan X Y and Hu F Q 2012 *IEEE Photon. Technol. Lett.* **24** 863
[5] Lv Q Q, Pan P, Ye H, Yin D D, Wang Y B, Yang X H and Han Q 2016 *Chin. Phys. B* **25** 038505
[6] Karagodsky V, Sedgwick F G and Chang-Hasnain C J 2010 *Opt. Express* **18** 16973
[7] Chang-Hasnain C J and Yang W J 2012 *Adv. Opt. Photon.* **4** 379
[8] Mateus C F R, Huang M CY, Chen L, Chang-Hasnain C J and Suzuki Y 2004 *IEEE Photon. Technol. Lett.* **16** 1676
[9] Ricciardi A, Campopiano S, Cusano A, Krauss T F and Faolain L O 2010 *IEEE Photon. J* **2** 696
[10] Zhou Y, Huang M C, Chase C, Karagodsky V, Moewe M, Pesala B, Sedgwick F G and Chang-Hasnain C J 2009 *IEEE J. Sel. Top. Quantum Electron* **15** 1485
[11] Tibuleac S and Magnusson R 1997 *Opt. Soc. Amer. A* **14** 1617
[12] Kanamori Y, Shhimono M and Hane K 2006 *IEEE Photon. Technol. Lett* **18** 2126
[13] Zhao H J, Peng Y J, Tan J, Liao C R, Li P and Ren X X 2009 *Chin. Phys. B* **18** 5326
[14] Fattal D, Li J J and Peng Z 2010 *Nat. Photon* **4** 466
[15] Lu F L, Sedgwick F G, Karagodsky V, Chase C and Chang-Hasnain C J 2010 *Opt. Express* **18** 12606
[16] Carletti L, Malureanu R, Mrk J and Chung I S 2011 *Opt. Express* **19** 23567
[17] Ma C L, Huang Y Q and Ren X M 2015 *Appl. Optics* **54** 973
[18] Duan X F, Zhou G R, Huang Y Q, Shang Y F and Ren X M 2015 *Opt. Express* **23** 2639
[19] Ma C L, Huang Y Q, Duan X F, D G D, M M and Ren X M 2015 *IEEE Photon. Technol. Lett.* **27** 679
[20] Vanbrabant P J M, Beeckman J, James R and Fernandez F A 2009 *Opt. Express* **17** 10895
[21] Moharam M G, Grann E B and Pommet D A 1995 *J. Opt. Soc. Am. A* **12** 1068